Inorg. Chem. **1986,** *25,* 283-287 **283**

Contribution from Ames Laboratory—DOE[1] and the Department of Chemistry,
Iowa State University, Ames, Iowa 50011

Synthesis and Structure of Double-Metal-Layered Scandium, Yttrium, and Zirconium Chloride Carbides and Nitrides, M_2Cl_2C and M_2Cl_2N

Shiou-Jyh Hwu, Robin P. Ziebarth, Samuel von Winbush, Jeff E. Ford, and John D. Corbett*

Received July 16, 1985

Syntheses are described for the isostructural 1T-M_2Cl_2C, M = Sc, Y, Zr, 1T-M'_2Cl_2N, M' = Sc, Zr, and 1T-Zr_2Br_2C from normal-valent halide, metal, and either graphite, N_2, NaN_3, or β-ZrNCl at 750–1000 °C in sealed Nb or Ta containers. All are formed in virtually quantitative yield save for Zr_2Cl_2N. The 1T-type structure, consisting of slabs of hcp layers sequenced X–M–M–X with C or N in trigonal-antiprismatic interstices between the double-metal layers, is related to that of ZrCl and ZrBr and is isostructural with Ta_2S_2C. The details of the structure were established from single-crystal studies of 1T-Sc_2Cl_2C and 1T-Sc_2Cl_2N (nitride: $P\bar{3}m1$, $Z = 1$, $a = 3.3495$ (4) Å, $c = 8.808$ (1) Å, $R = 0.050$ and $R_w = 0.060$ for 76 independent reflections, $2\theta < 50°$). Sc_2Cl_2C also occurs in a 3R-type arrangement of the same slabs. Alkali-metal intercalation of the scandium or zirconium chloride carbides was not successful. Reasons for the reordering of the ZrX host on bonding of interstitial C or N and XPS evidence for both the carbidic nature of carbon and a large M–C covalency in Sc_2Cl_2C and Zr_2X_2C are presented.

Introduction

The zirconium monohalides ZrCl[2-4] and ZrBr[5] provide a novel metal-like substrate for study. The structure consists of alternating pairs of cubic-close-packed layers of zirconium and halogen that are bonded together to produce tightly bound slabs in which four layers are sequenced X–Zr–Zr–X and orientated AbcA. These slabs are in turn weakly bound by van der Waals type interactions, stacking in the order ABC·· in ZrCl (designating the outer halogen layers only) or ACB·· in ZrBr and HfCl. The robust bonding within the double-metal layers by three electrons per metal produces very stable phases that are basically two-dimensional metals.

The same structures have been reported for ScCl,[6] YCl,[7,8] and many of the lanthanide chlorides and bromides,[9] although recent evidence is that all the monohalides of the trivalent elements are probably ternary phases stabilized by hydrogen.[10,11] In the cases of $TbClH_{0.8}$[12] and $YClH_x$,[11] hydrogen has been shown to reside in tetrahedral interstices between the double-metal layers in ZrX-type structures. At least some of the rare-earth-metal phases have a broad region of nonstoichiometry in hydrogen. These hydrides represent the first (but unrecognized) examples of a variety of interstitial derivatives of the ZrX-type substrate in which a non-metal is bound within the metal region. Oxide as ZrO_2 also reacts with ZrX to form the nonstoichiometric $ZrXO_z$ phases, $z \leq 0.43$ for chloride and ≤ 0.28 for bromide, with retention of the parent heavy-atom structure, oxygen randomly occupying tetrahedral voids between the metal layers.[13] The analogous reaction of "YCl" with oxygen provides a new layered form of YClO.[14] On the other hand, reaction of hydrogen with ZrX produces new structures in $ZrXH_{0.5}$ and ZrXH,[15,16] where hydrogen is located in distorted tetrahedra or in trigonal-antiprismatic (TAP) sites that are doubly occupied, respectively.[17]

This paper describes analogous phases involving interstitial carbon and nitrogen that are common to both group 3 (Sc, Y) and group 4 (Zr) elements. Some of these phases were first found serendipitously in low yields, and others, as a result of systematic exploration. A brief note on the carbides has appeared previously.[18] Analogous carbides as well as dicarbides of gadolinium[10,19] have also been reported, and many other examples of non-metals within isolated clusters[20] or in various metal-chain structures such as $Sc_7Cl_{10}C_2$[21] and Sc_4Cl_6B[22] have recently been obtained.

Experimental Section

Materials. The syntheses of the starting halides $ScCl_3$, YCl_3, $ZrCl_4$, and $ZrBr_4$, the preparation of the powdered metals from MH_2, the conduct of the reactions in sealed Nb or Ta tubing, and the Guinier and single-crystal X-ray methods have been described before.[5,14,21,23] β-ZrNCl was prepared according to Juza and Heners[24] from the reaction of $ZrCl_4$ and NH_3 at 600 °C. The scandium and yttrium metals were again prepared within Ames Laboratory while the zirconium was a reactor-grade crystal bar. The metals were typically cold-rolled and cut to strips ca. 0.5 × 5 × 10–30 mm. The ZrC and ZrN reactants were from CERAC, the graphite used was National spectroscopic powder from Union Carbide (in wt ppm: <1 ash, 0.8 Si, 0.5 Al, Fe, Na, ≤0.2 others), and the NaN_3 was from Aldrich. All materials were handled under drybox conditions; the nitride and carbide products are visibly sensitive to moist air over a period of several hours.

The stated new products were generally identified on the basis of a set of powder pattern data that refined to reproducible and consistent lattice constants in the appropriate crystal system and that exhibited intensities agreeing in detail with the distribution calculated for a known structure type or for the structure determined in the course of this research for Sc_2Cl_2Z, Z = C, N. Some small but regular deviations in intensities were observed and attributed to preferred orientation, a problem often encountered with layered materials because of the thin planar sample used in the Guinier method.

Lattice constants of the products were evaluated from Guinier photograph data (Cu $K\alpha_1$) by using NBS silicon as an internal standard combined with a least-squares fit of the standard's angles to their positions on the film and a subsequent least-squares refinement of the resulting 2θ–hkl data ($\lambda = 1.540\,56$ Å).

Carbides. The new phases are 1T-M_2X_2C for M = Sc, Y, Zr, X = Cl and some Br and 3R-Sc_2Cl_2C. In general, the reaction of stoichiometric amounts of the appropriate normal-valent halide, metal, and carbon provides the indicated product in greater than 95% yield. (A stated yield of >95% is a conservative interpretation of the absence of any other phase by Guinier powder photography.) The phases are generally very finely divided and sootlike and occur throughout the reaction container. The 3R-type scandium compound and the yttrium and zirconium phases are dark red-brown with a bronze reflectance under a

---

(1) Operated for the U.S. Department of Energy by Iowa State University under Contract No. W-7405-Eng-82. This research was supported by the Office of Basic Energy Sciences, Materials Sciences Division.
(2) Struss, A. W.; Corbett, J. D. *Inorg. Chem.* **1970**, *9*, 1373.
(3) Troyanov, S. I.; Tsirel'nikov, V. I. *Russ. J. Inorg. Chem.* (*Engl. Transl.*) **1970**, *15*, 1762.
(4) Adolphson, D. G.; Corbett, J. D. *Inorg. Chem.* **1976**, *15*, 1820.
(5) Daake, R. L.; Corbett, J. D. *Inorg. Chem.* **1977**, *16*, 2029.
(6) Poeppelmeier, K. R.; Corbett, J. D. *Inorg. Chem.* **1977**, *16*, 294.
(7) Mattausch, Hj.; Hendricks, J. B.; Eger, R.; Corbett, J. D.; Simon, A. *Inorg. Chem.* **1980**, *19*, 2128.
(8) Ford, J. E.; Meyer, G.; Corbett, J. D. *Inorg. Chem.* **1984**, *23*, 2094.
(9) Mattausch, Hj.; Simon, A.; Holzer, N.; Eger, R. *Z. Anorg. Allg. Chem.* **1980**, *466*, 7.
(10) Simon, A. *J. Solid State Chem.* **1985**, *57*, 2.
(11) Wijeyesekera, S. D.; Hwu, S.-J.; Corbett, J. D., to be submitted for publication.
(12) Ueno, F.; Ziebeck, K.; Mattausch, Hj.; Simon, A. *Rev. Chim. Miner.* **1984**, *21*, 804.
(13) Seaverson, L. M.; Corbett, J. D. *Inorg. Chem.* **1983**, *22*, 3202.
(14) Ford, J. E.; Corbett, J. D. *Inorg. Chem.* **1985**, *24*, 4120.
(15) Struss, A. W.; Corbett, J. D. *Inorg. Chem.* **1977**, *16*, 360.
(16) Marek, H. S.; Corbett, J. D.; Daake, R. L. *J. Less-Common Met.* **1983**, *89*, 243.
(17) Wijeyesekera, S. D.; Corbett, J. D. *Solid State Commun.* **1985**, *54*, 657.
(18) Ford, J. E.; Hwu, S.-J.; Corbett, J. D. *Inorg. Chem.* **1983**, *22*, 2789.
(19) Warkentin, E.; Masse, R.; Simon, A. *Z. Anorg. Allg. Chem.* **1982**, *491*, 323.
(20) Ziebarth, R. P.; Corbett, J. D. *J. Am. Chem. Soc.* **1985**, *107*, 4571.
(21) Hwu, S.-J.; Corbett, J. D.; Poeppelmeier, K. R. *J. Solid State Chem.* **1985**, *57*, 43.
(22) Hwu, S.-J.; Corbett, J. D., to be submitted for publication.
(23) Daake, R. L.; Corbett, J. D. *Inorg. Synth.* **1983**, *22*, 26.
(24) Juza, R.; Heners, J. *Z. Anorg. Allg. Chem.* **1964**, *332*, 159.

0020-1669/86/1325-0283$01.50/0 © 1986 American Chemical Society

strong light while the 1T-scandium phase is brown to black. Sufficient reaction conditions are 750–1000 °C for the scandium phases, 3 days at 950 °C being typical, and 950 °C for 5 and 10 days for the yttrium and zirconium compounds, respectively. The presence of a substoichiometric amount of carbon in the preparation of Sc_2Cl_2C, e.g. 50%, also produces $Sc_7Cl_{10}C_2$ as a second phase while the use of the latter as a reactant with stoichiometric amounts of Sc and C yields 1T-Sc_2Cl_2C directly. The 3R-type scandium compound is formed under the same conditions as the 1T structure but with either an excess of carbon ($\sim$5% or greater) or an excess of $ScCl_3$ with the proper proportions of Sc and C. No other ternary zirconium carbides are found up to 1150 °C by using the appropriate reaction stoichiometry; however, a 100% excess of carbon gives a very black, virtually amorphous and unknown material. No significant crystal growth was observed during the foregoing reactions.

Nitrides. Synthesis of the 1T-M_2Cl_2N phases, M = Sc, Zr, is more difficult because of the lack of a convenient and general nitrogen source. Only a limited amount of N_2 can be enclosed within the Ta or Nb container (which is usually welded under helium). For the scandium nitride, the decomposition of added NaN_3 in the presence of stoichiometric amounts of $ScCl_3$ and Sc powder at 735–860 °C for 5 weeks gave a >95% yield of the dark purple-red microcrystals (plus NaCl, presumably). The use of ZrNCl has proven to be a useful nitrogen source in the synthesis of zirconium clusters containing nitrogen.[20] Its reaction with excess $ZrCl_4$ and Zr powder at 850 or 900 °C for 29 or 21 days (but not at 950 °C, which gives ZrN and ZrCl) yielded a gray-black mixture of 1T-Zr_2Cl_2N and the less well-understood 3R-$ZrClN_x$ ($x \leq 1$) according to powder diffraction. (The latter has a 3R-$ZrBrO_x$ (condensed M_6X_8-type) structure,[13] not that of 1T- or 3R-Sc_2Cl_2C (condensed M_6X_{12}) of interest here, and probably involves nitrogen occupation of tetrahedral holes between the double-metal layers.) Use of NaN_3 in stoichiometric zirconium reactions at 850 °C gave the 1T compound plus ZrN in sizable amounts. Reactions of ZrCl contained in Mo or Ta boats within sealed SiO_2 containers with insufficient N_2 at 700 °C for 4–24 h produced mixtures of ZrN, β-ZrNCl, the 1T compound, and unreacted ZrCl.

Renewed attempts to prepare Zr_2Cl_2Z phases by the stoichiometric reaction of ZrCl, $ZrCl_4$, and ZrC or ZrN were frustrated by the oxide content of the samples of the last two, which instead produced mainly $ZrClO_x$.[13] The route is presumably feasible, but the reaction is very slow with such refractory and well-crystallized reactants.

The lack of reaction of ZrF_4 with ZrCl and Zr at 850–950 °C to form the analogous fluoride interstitial (or any other) compound was reconfirmed.[13] Attempts to intercalate Zr_2Cl_2C with Na, K, Ca, Cu, or Ag at 850–1270 °C or with Na in liquid NH_3 or to intercalate Sc_2Cl_2C with Na at high temperatures were all unrewarding. 1T-Zr_2Cl_2C does not react with H_2 at 350 °C and 1 atm.

Photoelectron Spectra. The X-ray (XPS) data were secured with Al Kα radiation and an AEI ES200B spectrometer coupled with a Nicolet 1180 minicomputer for averaging, as before.[25] Generally, 50–500 scans were made by utilizing 512 channels. Samples were opened, ground, and mounted on In foil within a helium-filled drybox that was attached directly to the sample chamber of the spectrometer and maintained at <1 ppm O_2 and <0.5 ppm H_2O. Calibration was provided by adventitious carbon at 285.0 eV.

Single-Crystal Studies. Crystals of what turned out to be 1T-Sc_2Cl_2C and 1T-Sc_2Cl_2N were obtained as the result of accidental impurities prior to the direct syntheses just described. A few black crystals of the nominal carbide were found in the hot end (along with 10% $Sc_7Cl_{10}C_2$) from a 4-week, 1000/980 °C gradient reaction of $ScCl_3$ and ScOCl (4:3) and excess Sc strips. Dark purple-red nitride crystals likewise were obtained from the hot end of a 5-week, 830/810 °C reaction of Sc powder, $ScCl_3$, and CsCl. Products at the cold ends in the two reactions were respectively ScOCl plus $ScCl_3$ and what had been a melt at temperature, typically $Cs_3Sc_2Cl_9$ and $CsSc_{1-x}Cl_3$. Zero- and first-level Weissenberg photographs of the nitride crystals indicated a hexagonal cell with dimensions appropriate to a one-slab structure and with no systematic extinctions. Data were collected at room temperature on a four-circle Ames Laboratory diffractometer equipped with a monochromator and with the aid of Mo radiation (λ = 0.710 34 Å). Crystal, data collection, and refinement parameters are listed in Table I. Programs for data averaging, absorption correction, Fourier synthesis and refinement, and the sources of scattering factors (including anomalous dispersion corrections) were as referenced before.[4,14]

The appropriate model for a close-packed arrangement of heavy-atom layers was the yttrium and chloride positions that had been deduced just previously[18] for $K_{0.5}Y_2Cl_2C$ in space group $P\bar{3}m1$. Such refined well for both scandium crystals but also left residual densities of $Z \sim 5$ (C) or 5.8 (N) e/Å^3 in the trigonal-antiprismatic holes between the scandium layers (0, 0, $^1/_2$) while any residuals elsewhere were <1 e/Å^3. Inclusion of the indicated interstitial atoms (selected on the basis of dimensional arguments below) allowed simultaneous and reasonable refinement of both the occupancies and the isotropic *B* values (Table I; $w = \sigma_F^{-2}$). Final difference maps were flat to <0.5 e/Å^3.

Table I. Crystal and Refinement Data for 1T-Sc_2Cl_2Z, Z = C or N[a]

	Sc_2Cl_2C	Sc_2Cl_2N
cryst size, mm	0.20 × 0.16 × 0.05	0.20 × 0.18 × 0.05
latt const (diffr[b])		
a, Å	3.3997 (8)	3.3495 (4)
c, Å	8.858 (3)	8.808 (1)
no. of reflcns		
measd	436	424
obsd[c]	362	374
indep	73	76
R_{av}	0.053	0.049
R/R_w,[d] %	3.5/5.3	5.0/6.2
μ, cm^{-1}	50	53
transm coeff	0.70–1.00	0.77–0.98
interstitial atom	C	N
occupancy	1.18 (7)	1.10 (4)
B, Å^2	2.1 (4)	1.7 (4)
R/R_w (final), %	3.2/5.0	5.0/6.0

[a] Space group $P\bar{3}m1$, $Z = 1$; Ω scan, $2\theta_{max} = 50°$. [b] Experience has shown that the diffractometer gives lattice constants 0.05–0.1% lower than from Guinier methods. [c] One hemisphere, $F_o > 3\sigma_F$, $I_o > 3\sigma_I$. [d] $R = \sum||F_o| - |F_c||/\sum|F_o|$; $R_w = [(\sum w(|F_o| - |F_c|))^2/\sum w|F_o|^2]^{1/2}$; unit occupancy for *Z*.

Results

The new phases identified in the course of this work again[14,21] followed a structural solution for and some detective work on single crystals of two reduced scandium chlorides that were unexpectedly obtained in low yields. Both turned out to be stabilized by second-period impurity atoms. The work followed closely on the deduction of the basic structure of a 1T phase $K_xY_2Cl_2Z$ with the same AbaB layering of heavy atoms in a one-slab host structure and with an unknown Z in a trigonal-antiprismatic cavity between the metal layers. The size of the interstitial cavities in all three of these and the refined scattering power of this atom in the scandium pair led to the postulate that Z was carbon in the first two phases discovered and nitrogen in the third. Such elements were subsequently employed in preparation of the same phases in high yield, the correspondence being established mainly by comparison of precise lattice constants. (The same sequence of reasoning also led to the subsequent syntheses of $M_{0.5}Y_2Cl_2C$, M = Li–K, Cs.[18]) Although the heavy-atom layering in the 1T-type host structures can be deduced from powder data alone, identification of the location of the interstitial is more satisfactory when based on direct refinement rather than inference. On the other hand, the zirconium monohalide reactions leading to the carbide and nitride described herein were part of a systematic follow-up on earlier[13] unsuccessful reactions of ZrCl with ZrC and ZrN as the sources of the interstitial nonmetals.

The crystal structure parameters and some distances for Sc_2Cl_2C and Sc_2Cl_2N are given in Table II while the structure factor data are available as supplementary material. The anisotropic thermal parameters are also included in Table II as these are particularly significant regarding the crystal and refinement quality for such infinite-layered materials that are frequently laden with stacking defects. The occupancy and the isotropic temperature factor of the light atom could be simultaneously refined with both crystals to obtain some idea of its identity. These occupancies converged at 1.18 (7) for carbon and 1.10 (4) for nitrogen, respectively. In addition, the purple-red color of the nitride single crystal was unmistakably the same as that of the known nitride, and the same was true of lattice constants determined on the diffractometer (Table I) relative to those from Guinier techniques both for the same reaction product and for later preparations with known non-metal interstitial (Table III). On the other hand, the so-called carbide single crystal gave appreciably smaller lattice parameters than the reference powdered carbide, and interpolation

---

(25) Corbett, J. D.; Meyer, G.; Anderegg, J. W. *Inorg. Chem.* **1984**, *23*, 2625.

Table II. Atom Parameters in and Selected Distances for 1T-Sc_2Cl_2C and 1T-Sc_2Cl_2N, Space Group $P\bar{3}m1$[a]

Atom Parameters

	1T-Sc_2Cl_2C			1T-Sc_2Cl_2N		
	z	B_{11}	B_{33}	z	B_{11}[a]	B_{33}
Sc (2d)	0.3629 (2)	0.93 (8)	1.38 (10)	0.3656 (2)	0.86 (10)	0.82 (11)
Cl (2d)	0.8249 (3)	1.25 (10)	1.55 (11)	0.8242 (3)	1.10 (10)	0.98 (12)
Z (1b)	0.5	1.3 (3)[b]		0.5	1.2 (3)[b]	

Distances (Å)

	1T-Sc_2Cl_2C	ScCl[c]	1T-Sc_2Cl_2N
	Interlayer		
Sc–Sc	3.123 (3)	3.216 (6)	3.057 (3)
Sc–Cl	2.573 (2)	2.591 (4)	2.556 (2)
Cl–Cl	3.671 (5)	3.695 (8)	3.651 (5)
Cl–Z	3.484 (2)		3.449 (2)
Sc–Z	2.308 (1)		2.267 (1)
	Intralayer		
Sc–Sc, Cl–Cl	3.3997 (8)	3.473 (2)	3.3495 (4)

[a] $T = \exp[(-^1/_4(B_{11}h^2a^{*2} + B_{22}k^2b^{*2} + B_{33}l^2c^{*2} + 2B_{12}hka^*b^* + 2B_{13}hla^*c^* + 2B_{23}klb^*c^*)]$; $B_{11} = B_{22}$, $B_{12} = B_{13} = B_{23} = 0$. [b] Unit occupancy of interstitial atoms, corresponding to the first set of R values in Table I. [c] Reference 6.

Table III. Lattice Constants of Carbides and Nitrides from Guinier Powder Data (Å)[a]

	a	c	V, Å^3	no. of lines
Sc_2Cl_2C (1T)	3.4330 (7)	8.916 (4)	90.91 (5)	11
Sc_2Cl_2C (3R[b])[c]	3.4354 (2)	8.868 (1)	90.64 (2)	15
Sc_2Cl_2N (1T)	3.3517 (7)	8.813 (2)	85.74 (6)	17
Y_2Cl_2C (1T)	3.7051 (5)	9.183 (2)	109.17 (5)	22
Zr_2Cl_2C (1T)	3.4229 (4)	8.987 (6)	91.19 (8)	11
Zr_2Br_2C (1T)	3.4883 (6)	9.431 (3)	99.38 (5)	14
Zr_2Cl_2N (1T)	3.4114 (3)	8.837 (2)	88.97 (3)	14
ZrCl (3R)[c]	3.4233 (5)	8.898 (1)	90.30 (4)	10
ZrBr (3R)[c]	3.5031 (3)	9.357 (1)	99.44 (3)	23

[a] Space groups: 1T, $P\bar{3}m1$; 3R, $R\bar{3}m$. [b] Ab(c)aB layer stacking as in the 1T type; 3R–ZrX is AbcA. [c] $c/3$ and $V/3$ for comparison; ZrX data from ref 13.

suggests that perhaps 60% carbon, the balance nitrogen, could have been incorporated in the accidental synthesis that produced the single crystal. We have had no success incorporating oxygen in any of these hosts, (Sc,Y)OCl or $ZrXO_z$[13] being the preferred products.

Syntheses of the phases M_2Cl_2C for M = Sc, Y, Zr, M'_2Cl_2N for M′ = Sc, Zr, and Zr_2Br_2C from normal-valent halides, metal, or either graphite, N_2, NaN_3, or ZrNCl generally proceed directly, with high yields. Guinier lattice parameters are summarized in Table III, while powder pattern data for 1T types Sc_2Cl_2C, Sc_2Cl_2N, and Y_2Cl_2C are in the supplementary material. The zirconium reaction involves an oxidation of the metal in the ZrX substrate from +1 to +2.5 (N) or +3 (C). The Zr_2Cl_2N synthesis in particular is somewhat more difficult because of the high autogeneous disproportionation pressure of $ZrCl_4$ that develops at temperatures necessary for the reaction of N_2 with ZrCl in open systems, this decomposition yielding ZrN as a byproduct. The general success of these reactions must depend in part on the effective inertness of the Ta or Nb containers to carbon or nitrogen together with some means of transporting carbon. The former probably depends mainly on the greater thermodynamic stability of zirconium (and probably Y and Sc) carbides and nitrides although a low diffusion coefficient of these non-metals in Ta and Nb probably also helps in limiting any intermediate reaction to a surface coating.

There is no evidence for nonstoichiometry in Zr_2Cl_2C judging from its lattice constants, which seemed to be invariant under all sorts of conditions. On the other hand, a small dimensional variation is detectable with 1T-Sc_2Cl_2C, a deficiency of carbon leading to c axial lengths perhaps 0.02–0.03 Å lower than those given in Table II or a moderate excess of carbon or excess scandium combined with long equilibration at high temperature tending to give higher values for the c lattice constant, up to 9.06 Å. The dimensional data for 3R-Sc_2Cl_2C seem to be quite invariant. The yttrium and nitrogen systems were not investigated in this respect.

Discussion

The M_2X_2C and M_2Cl_2N phases are isostructural and, for the zirconium carbides and scandium nitride, isoelectronic with Ta_2S_2C, a phase that also occurs in the 1T and 3R structures[26] as does Sc_2Cl_2C. The 3R type is better known as the Bi_2Te_2S (tetradymite) structure[27] and is obtained for the tantalum phase by annealing at 1250 °C. No transformation between the two analogous scandium phases could be accomplished up to 1000 °C while 1T-Zr_2Cl_2C showed no change to 1150 °C. Neither the zirconium nor the scandium chloride carbides could be intercalated although 1T-$M_xY_2Cl_2C$ phases as well as 2H- and 3R-$M^I_xTa_2S_2C$[28] are known. These are all based on the same hcp heavy-atom slabs. The structures deduced for the 2H- and 3R-tantalum intercalates are unusual in that they all show second-nearest-neighbor M^I–Ta interactions of the sort that appear to be avoided in analogous chloride hydride, and carbide systems for the rare-earth metals.[10,11,14,18]

The cell volumes and distances found in the scandium and yttrium derivatives (Tables II and III) attest to the strength of the bonding relative to that in "ScCl" and "YCl", the latter actually being $MClH_{\sim 0.5}$ phases with hydrogen in tetrahedral holes between the double-metal layers in ZrX-type structures.[10-12] The decrease in the Sc–Sc separations on the formation of the carbide is on the order of 0.07–0.09 Å. The more strongly bound zirconium monohalide parent phases undergo either a moderate expansion or contraction, particularly in c, on a formation of the carbide or the nitride, respectively. The difference in cell volumes between the 1T- and the 3R-Sc_2Cl_2C phases is relatively small, in the opposite direction from the similarly small difference found in the isostructural pair of Ta_2S_2C phases.[26,28]

Figure 1 illustrates by means of [110] sections[29] the layering sequence in one slab of the 3R-ZrX phases (left) and in the 1T-type structure of Sc_2Cl_2N (right) that is common to all of the phases reported herein. The structural rearrangement of the AbcA

---

(26) Beckmann, O.; Boller, H.; Nowotny, H. *Monatsh. Chem.* **1980,** *101,* 945.

(27) Hulliger, F. "Structural Chemistry of Layer-Type Phases"; Lêvy, F., Ed.; D. Reidel Publishing Co: Boston, 1976; p 197.

(28) Brec, R.; Ritsma, J.; Ouvard, G.; Rouxel, J. *Inorg. Chem.* **1977,** *16,* 660.

(29) Hexagonal nets that are close packed in any sequence are conventionally described in terms of A, B, or C representations of their relative orientation in projection. This description also may be used for interstitial atoms in tetrahedral, octahedral, or trigonal-prismatic orientation between the layers. The [110] sections of such structures are very convenient pictorials since all atoms lie on such planes.

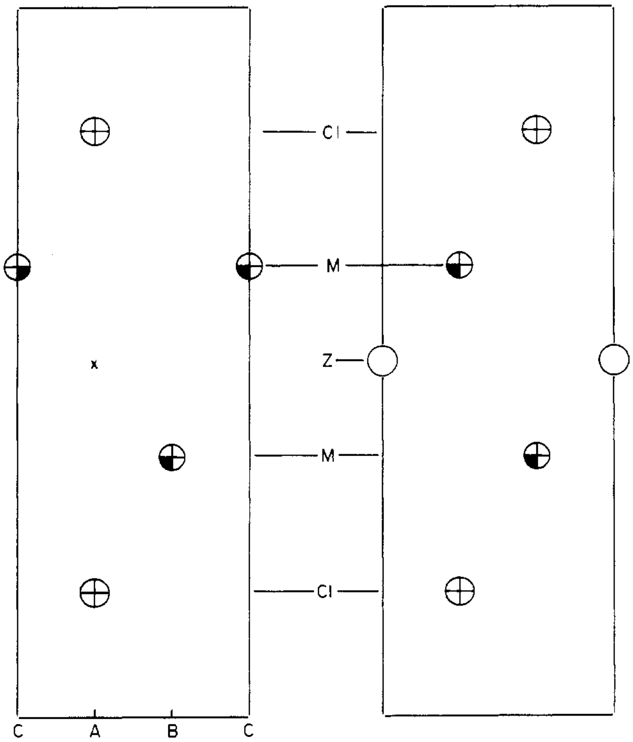

Figure 1. The [110] section for each slab in the ZrX structure (left, schematic) and in the 1T structure typified by 1T-Sc_2Cl_2N (right, 90% probability thermal ellipsoids). The layers are horizontal, and the *c* axis is vertical. The small × marks the trigonal-antiprismatic site in ZrX. Crossed figures are chlorine, shaded ellipsoids are metal, and open circles are nitrogen or carbon.

Table IV. XPS Core Binding Energy Data (eV)[a]

substance	Sc $2p_{3/2}$	Cl $2p_{3/2}$	C 1s	carbon shift	Sc 2p–Cl 2p
Sc	398.7				
Sc_7Cl_{10}	398.8	200.2			198.6
$Sc_7Cl_{10}C_2$	401.0	199.9	281.9	-3.1	201.1
Sc_2Cl_2C	400.8	200.0	282.0	-3.0	200.8
$ScCl_3$	404.0	200.1			203.9
substance	Zr $4d_{5/2}$	Cl $2p_{3/2}$	C 1s	carbon shift	Zr 4d–Cl 2p
Zr	178.5				
ZrCl	179.4	199.6			-20.2
Zr_2Cl_2C	180.2	200.0	282.8	-2.2	-19.8
$ZrCl_2$[b]	180.2	200.0			-19.8
$ZrCl_3$	182.2	199.7			-17.5
$ZrCl_4$	182.8	198.5			-15.7
substance	Zr $4d_{5/2}$	Br $3p_{1/2}$	C 1s	carbon shift	Zr 4d–Br 3p
ZrBr	180.0	190.4			-10.4
Zr_2Br_2C	180.1	190.5	282.8	-2.2	-10.4

[a] Based on adventitious C 1s ≡ 285.0 eV. Data for those other than M_2X_2C and ZrBr are from ref 21 and from: Cisar, A. J.; Corbett, J. D.; Daake, R. L. *Inorg. Chem.* **1979**, *18*, 836. [b] 3R-MoS_2 type.

order of the layers in ZrX (or (Sc,Y)$ClH_{0.5}$) (Figure 1, left) into the AbaB sequence of the 1T structures on bonding of carbon or nitrogen into trigonal-antiprismatic holes (right) appears to be a logical consequence of what would otherwise be excessively short, second-nearest-neighbor interactions between interstitial (at *x*) and halide along the *c* axis. There may be electronic factors involved as well. The change in halide positioning may also be viewed as a conversion from condensed M_6X_8- to M_6X_{12}-type clusters, left and right, respectively, in Figure 1. This exclusion of face-capping (M_6X_8) halide when the centers of metal octahedra (TAP) are occupied by interstitials (other than H) appears to be a common effect in many compounds of this character, the conversion of infinite chains of double-metal octahedra that are face-capped by halide in Sc_7Cl_{10} to edge-bridging halide in $Sc_7Cl_{10}C_2$[21] being just one example.[10] It should be noted that the 3R version of Sc_2Cl_2C (and Ta_2S_2C) involves just a rhombohedral stacking of the above 1T-type slabs while 3R-$ZrClZ_x$, Z = O, N, and 3R-$MClH_x$, M = Tb, Y (and probably Sc), involve M_6X_8 parentage with the interstitials in *tetrahedral* holes. In contrast, however, the higher electron count and increased Zr–Zr bonding in the ZrX matrix evidently require that the formation of ZrXH include a transformation to AbaB stacking so that *pairs* of hydrogen atoms can now be placed within each trigonal antiprism.[11,17]

The interaction of carbon with the hypothetical ScCl or the real ZrCl matrix in forming these compounds is by all measures very strong, and the classical definition of "interstitial" as a fairly weakly interacting atom filling a more-or-less preexisting hole seems very inappropriate. We will later describe extended Hückel calculations together with UPS data that well illuminate the sizable electronic reorganization and energetic changes brought on by such non–metal atoms in these monohalides and in other lattices.[30] Evidence is already on hand for what turn out to be remarkably similar effects on the binding of carbon etc. within octahedral metal clusters such as $[Zr_6X_{12}C]X_2$, X = Cl, I, where the metal–metal bonding is somewhat more localized.[20,31] As expected, the carbon s and p valence orbitals interact strongly with cluster orbitals of the same symmetry to form lower lying $a_{1g}{}^2$ and $t_{1u}{}^6$ levels at ∼-14 and -4 eV relative to the $t_{2g}{}^6$ HOMO, which is mainly Zr–Zr bonding. Strong Zr–C covalency is an important part of this reorganization, and the carbon charges must be negative but low, perhaps -0.5 to -1.0 based on detailed calculations for rock-salt monocarbides.[32] The low charge on carbon that derives from this covalency contrasts with the conventional oxidation state assignment of -4 that goes with filling of the carbon valence orbitals (or band). The latter convention leads to a +3 oxidation state assignment for the metal in Sc_2Cl_2C while, coincidentally, both Zr_2Cl_2C and the above $Zr_6Cl_{14}C$ are formally zirconium(III) compounds. These assignments are still useful and consistent with the apparent semiconducting character of Sc_2Cl_2C and the metal-like behavior of Zr_2Cl_2C that are indicated by both valence structure (UPS) measurements and extended Hückel calculations.[30]

A carbidic nature of carbon and the M–C covalency can both be inferred from the XPS core binding energies for the carbon and metal listed in Table IV. The 1s level of metal-bonded carbon in these and related phases is found to be shifted to lower binding energies from that of the adventitious carbon (hydrocarbon) calibrant, by 3.0 eV in Sc_2Cl_2C, 3.1 eV in $Sc_7Cl_{10}C_2$,[21] and 2.2 eV in the evidently less polar Zr_2X_2C, X = Cl, Br. These shifts are indicative of a more negative, anionic state for carbon but should not be taken to imply an ionic bonding.

The dependency of metal-core shift on oxidation state and on the non-metal is clearly indicative of a sizable covalency. The well-known increase in core binding energies with increasing oxidation state for transition metals especially is normally developed for a series of compounds with a fixed non-metal. However, even this trend may be confused by significant and unpredictable variations in the Fermi energy to which these data on the solids are presumed to be referenced. In such cases, referencing of the metal-core energies to an internal anion or ligand standard is much clearer.[25] Such data relative to halide are shown in the last column of Table IV, although the internal references is really necessary only for the zirconium series.[33]

The progression to higher relative metal binding energies seen in the $ZrCl_n$ series, *n* = 1, 2, 3, 4, clearly does not apply to zirconium(III) in Zr_2Cl_2C where the metal binding energy is the same as in $ZrCl_2$ rather than a 2.3 eV smaller value for the analogous $ZrCl_3$. In fact, no change in the relative zirconium core

---

(30) Ziebarth, R. P.; Hwu, S.-J.; Corbett, J. D. *J. Am. Chem. Soc.*, in press.

(31) Smith, J. D.; Corbett, J. D. *J. Am. Chem. Soc.* **1985**, *107*, 5704.

(32) For example, see: Neckel, A. *Int. J. Quantum Chem.* **1983**, *23*, 1317.

(33) Corbett, J. D. *Inorg. Chem.* **1983**, *22*, 2669.

energy is seen on oxidizing ZrBr to Zr_2Br_2C while scandium(III) in Sc_2Cl_2C differs from that in $ScCl_3$ by a remarkable 3.2 eV. Similar effects have been reported for $Sc_7Cl_{10}C_2$,[21] where the scandium oxidation state in the metal chain is +2.5, and for ZrH_2 and ZrClH relative to $ZrCl_2$.[16] These differences must arise from the greater covalency (lower polarity) of the metal–carbon bonds relative to the metal–halogen bonds. It could be argued that final-state relaxation effects are responsible for up to half of the difference seen with Zr_2Cl_2C, but this is clearly less plausible for the filled-band Sc_2Cl_2C.

Acknowledgment. The authors wish to express their appreciation to Prof. R. A. Jacobson for provision of the single-crystal X-ray diffraction facilities and to J. W. Anderegg for the XPS measurements. Samuel von Winbush was supported as a DOE Faculty Research Participant.

Registry No. Sc_2Cl_2C, 97005-30-6; Sc_2Cl_2N, 99654-89-4; Y_2Cl_2C, 99665-56-2; Zr_2Cl_2C, 99665-57-3; Zr_2Br_2C, 99665-58-4; Zr_2Cl_2N, 99654-90-7; $ScCl_3$, 10361-84-9; YCl_3, 10361-92-9; $ZrCl_4$, 10026-11-6; $ZrBr_4$, 13777-25-8; Sc, 7440-20-2; Y, 7440-65-5; Zr, 7440-67-7; N_2, 7727-37-9; NaN_3, 26628-22-8; ZrNCl, 13932-08-6; C, 7440-44-0; graphite, 7782-42-5.

Supplementary Material Available: Listings of observed and calculated structure factor data for Sc_2Cl_2Z, Z = C, N, and the Guinier powder patterns of 1T-Sc_2Cl_2C, -Sc_2Cl_2N, and -Y_2Cl_2C (4 pages). Ordering information is given on any current masthead page.

Contribution from the Department of Chemistry and Laboratory for Molecular Structure and Bonding,
Texas A&M University, College Station, Texas 77843

Oxidative Addition of Diphenyl Disulfide across a Ta=Ta Bond. Preparation and Characterization of $[TaCl_3(Me_2S)]_2(\mu\text{-}SPh)_2$

Gordon C. Campbell, Jo Ann M. Canich, F. Albert Cotton,* Stan A. Duraj, and James F. Haw

Received August 30, 1985

The tantalum complex $(SMe_2)Cl_2Ta(\mu\text{-}Cl)_2(\mu\text{-}SMe_2)TaCl_2(SMe_2)$, possessing a $\sigma^2\pi^2$ Ta=Ta double bond, reacts readily with PhSSPh to give $(SMe_2)Cl_3Ta(\mu\text{-}SPh)_2TaCl_3(SMe_2)$. In this reaction, the starting material loses the bridging SMe_2 ligand and two chloride bridges are broken while only two new SPh bridges are formed in the final product. This oxidative-addition reaction of the S—S single bond to the Ta=Ta double bond converts the face-sharing bioctahedron structure of the starting compound to an edge-sharing bioctahedron structure in the final dimer, with concomitant change of the oxidation state of tantalum from III to IV. The product is the first example of a d^1–d^1 ditantalum thiolate-bridged dimer. Important structural data for $(SMe_2)Cl_3Ta(\mu\text{-}SPh)_2TaCl_3(SMe_2)$, which has an inversion center, are as follows: Ta–Ta distance, 3.165(1) Å; Ta–S(SMe_2), 2.707 (2) Å; Ta–S(μ-SPh), 2.372 (2) Å for sulfur trans to SMe_2 ligand; Ta–S(μ-SPh), 2.448 (2) Å for sulfur trans to Cl(2) atom; Ta–Cl(1) and Ta–Cl(3), 2.328 (2) and 2.331 (2) Å, respectively; Cl(1) and Cl(3) atoms located above and below the $Ta(\mu\text{-}SPh)_2Ta$ parallelogram plane. The new compound crystallizes in the monoclinic space group $C2/c$ with a = 17.934 (5) Å, b = 12.445 (4) Å, c = 11.705 (4) Å, β = 92.50 (3)°, V = 2610 (2) Å^3, and Z = 4. Solid-state ^{13}C NMR spectroscopy with cross polarization and magic-angle spinning (CP/MAS) at 28 and −103 °C provides evidence that this compound is diamagnetic, which is in accord with the results of a Fenske–Hall calculation predicting a single bond for the tantalum–tantalum d^1–d^1 pair.

Introduction

Complexes possessing multiple metal–metal bonds, which may be viewed as units of unsaturation containing metal atoms in lower oxidation states, are usefully reactive. This can be illustrated by several previously reported oxidative-addition reactions that these complexes undergo. The following are representative:

$$Mo_2Cl_4(dppe)_2 + EtSSEt \rightarrow (dppe)Cl_2Mo(\mu\text{-}SEt)_2MoCl_2(dppe)^{1}$$

$$Mo_2(O\text{-}i\text{-}Pr)_6 + i\text{-}PrOO\text{-}i\text{-}Pr \rightarrow Mo_2(O\text{-}i\text{-}Pr)_8{}^{2}$$

$$Mo_2(O\text{-}i\text{-}Pr)_6 + 2Cl_2 \rightarrow Mo_2(O\text{-}i\text{-}Pr)_6Cl_4{}^{2}$$

$$Nb_2Cl_6(Me_2S)_3 + PhN{=}NPh \rightarrow Nb_2Cl_6(Me_2S)_2(NPh)_2{}^{3}$$

$$W_2(OCMe_3)_6 + PhNO \rightarrow [W(OCMe_3)_2(NPh)]_2(\mu\text{-}O)(\mu\text{-}OCMe_3)_2{}^{4}$$

We are currently conducting a broadly based systematic study of oxidative addition reactions involving double, triple, and quadruple bonds between metal atoms with the objective of providing generally useful, predictable synthetic chemistry. One class of starting materials that figure prominently in our program comprises the dinuclear, doubly metal–metal-bonded compounds of niobium and tantalum, of general formula $M_2X_6L_3$. Those most commonly used by us are the ones with X = Cl and L = Me_2S, Et_2S, or $(CH_2)_4S$. In this paper, we report the reaction of $Ta_2Cl_6(Me_2S)_3$ with PhSSPh, to give a dinuclear, Ta–Ta bonded product in which the PhSSPh reagent has reacted to give two μ-SPh groups. The product has been characterized by X-ray crystallography and solid-state ^{13}C NMR spectroscopy, and the electronic structure has been examined by means of a molecular orbital calculation.

Experimental Section

All manipulations were carried out under an atmosphere of argon. Standard Schlenk and vacuum-line techniques were used. Benzene and hexane were freshly distilled from benzophenone ketyl prior to use. Solutions and solvents were transferred via stainless-steel cannulae and/or syringes. Diphenyl disulfide was purchased from Eastman and was deaerated under vacuum at room temperature. $Ta_2Cl_6(Me_2S)_3$ was prepared according to a literature procedure.[5] The IR spectrum was recorded on a Perkin-Elmer 783 spectrophotometer. Elemental analyses were performed by Galbraith Laboratories, Inc.

Solid-state, 25.02-MHz ^{13}C CP/MAS (cross polarization and magic-angle spinning) NMR spectra of ca. 400 μL (ca 0.9 g.) of $[TaCl_3(Me_2S)]_2(\mu\text{-}SC_6H_5)_2$ were obtained in a Kel-F rotor on a Chemagnetics spectrometer. The matched spin-lock contact time was 1 ms, and 2000 scans were acquired per spectrum. All chemical shifts were measured relative to tetramethylsilane by using hexamethylbenzene as a secondary substitution reference. The sample rotor was packed in a Vacuum Atmospheres drybox and magic-angle spinning was performed with dry nitrogen in order to avoid contacting the sample with air or moisture.

---

(1) Cotton, F. A.; Diebold, M. P.; O'Connor, C. J.; Powell, G. L. *J. Am. Chem. Soc.* **1985**, *107*, 7438.

(2) Chisholm, M. H.; Kirkpatrick, C. C.; Huffman, J. C. *Inorg. Chem.* **1981**, *20*, 871.

(3) Cotton, F. A.; Duraj, S. A.; Roth, W. J. *J. Am. Chem. Soc.* **1984**, *106*, 4749.

(4) Cotton, F. A.; Shamshoum, E. S. *J. Am. Chem. Soc.* **1984**, *106*, 3222.

(5) Cotton, F. A.; Najjar, R. C. *Inorg. Chem.* **1981**, *20*, 2716.

0020-1669/86/1325-0287$01.50/0